Materials Today Bio 32 (2025) 101686

Contents lists available at ScienceDirect

Materials Today Bio

journal homepage: www.journals.elsevier.com/materials-today-bio

Bioactive multifunctional hydrogels accelerate burn wound healing via M2 macrophage-polarization, antioxidant and anti-inflammatory

Erman Zhao [a], Xiuling Tang [a], Xitong Li [b], Jun Zhao [a], Saiying Wang [a], Gaofei Wei [c,*], Le Yang [a,**], Minggao Zhao [a,***]

[a] Precision Pharmacy & Drug Development Center, Department of Pharmacy, Tangdu Hospital, Air Force Medical University, Xi'an, 710038, China
[b] Department of Surgery, Xi'an Lintong District People's Hospital, Xi'an, 710600, China
[c] Institute of Medical Research, Northwestern Polytechnical University, Xi'an, 710072, China

ARTICLE INFO

Keywords:
Angiogenesis
Anti-inflammation activity
Macrophages polarization
Multifunctional hydrogels
Burns
Antibacterial

ABSTRACT

Globally, more than 300,000 fatalities occur from burns annually, and burn-wound healing continues to present significant challenges owing to the wound's propensity for infections, heavy bleeding, poor angiogenesis, and persistent inflammatory responses. The immunomodulation of macrophage polarization toward the M2 phenotype facilitates the healing of burn wounds by controlling the tissue microenvironment and expediting the transition from the inflammatory phase to proliferation. Here, a polydopamine-mediated graphene oxide (GA), tannic acid (TA), and magnesium ion (Mg^{2+})-incorporated multifunctional gelatin (Gel) scaffold (GTMG) is developed to accelerate wound healing by modulating the inflammatory microenvironment of burn wounds. GA and Mg^{2+} confer the scaffold with the conversion of M1-type to M2-type macrophages and vascular regeneration. TA and GA synergistically provide with antimicrobial capabilities to the hydrogel. Additionally, the multifunctional hydrogel shows strong hemostatic, anti-inflammatory and biocompatible properties. Due to its strong tissue adhesion and injectability, the hydrogel can also be used for various forms of dynamic burn wounds. *In vivo* research shows that the hydrogel may have hemostatic, anti-inflammatory, and M2-phenotypic macrophage-polarization effects, which increase the regeneration and repair effects of burn sites and shorten the burn-healing time. The results indicate that this multifunctional hydrogel offers a promising therapeutic approach for the treatment of burn wounds by altering the immunological microenvironment and accelerating the three phases of wound healing.

1. Introduction

According to the World Health Organization, burns affect millions of people and cause more than 300,000 deaths annually. Deep burns result in tissue damage, large irregularly shaped wounds, severe bleeding, increased susceptibility to wound infection, and accelerated production of free radicals [1,2]. In addition, inflammatory cytokines are overexpressed in the wound microenvironment owing to epithelialization dysfunction and the long-term inflammatory state of burn wounds. Delaying the healing process of the wound from the inflammation to proliferation-phase leads to difficulty in wound healing, which may lead to sepsis or even be life-threatening in severe cases [3–7]. The primary cause of chronic inflammatory excess burns results in a dysregulated macrophage response with an impaired phenotypic transition from an inflammatory (M1) to an anti-inflammatory (M2) state [8–10]. Our previous studies have shown that the M2-type macrophages not only contribute to tissue repair and reduce inflammation, but they also release angiogenic substances such as vascular endothelial growth factor (VEGF), which is essential for revascularization. In contrast, an excessive inflammatory response severely disrupts blood-flow reconstruction and tissue regeneration in wounds [11–13]. Although various clinical treatments have been developed to treat burn wounds, including skin grafts, dressings, and medications, the long hospitalization time required for patients and high cost of surgery make burn treatments unsatisfactory [14–16]. Therefore, novel and affordable therapeutic methods, such as multifunctional biomaterial dressings that modulate

* Corresponding author.
** Corresponding author.
*** Corresponding author.
E-mail addresses: weigf0605@163.com (G. Wei), yanglefmmu@163.com (L. Yang), minggao@fmmu.edu.cn (M. Zhao).

https://doi.org/10.1016/j.mtbio.2025.101686
Received 17 December 2024; Received in revised form 5 March 2025; Accepted 19 March 2025
Available online 27 March 2025

chronic inflammation and angiogenic disorders in burn wounds, may be widely applied to accelerate the healing of burn wounds.

Currently, hydrogels are considered as the most promising wound dressings because they possess a hydrophilic three-dimensional (3D) network structure that facilitates oxygen exchange, creates a breathable and moist environment for wounds by absorbing the excess wound exudate, and provides a suitable delivery system for cells and other biomolecules to promote wound healing [17–21]. However, traditional hydrogel dressings currently available in the market are unable to meet the required characteristics for wound healing; they exhibit a low degradation rate, single functionality, and an inability to adapt to irregularly shaped wounds [14–16]. The ideal wound dressing should have a variety of functions to meet different pathological conditions. Recently, many efforts have been devoted to develop multifunctional hydrogel for skin wound healing. For example, Zhang et al. designed a hydrogel with a "Pull−Push" Approach, integrating antibacterial and anti - inflammatory functions to jointly promote wound healing [17]. Chen et al. designed a multifunctional fibrin gel, which demonstrated good local analgesic effects, as well as rapid hemostasis, anti-inflammatory and antibacterial functions, accelerating the wound closure time [18].

The immune system plays a crucial role in the regeneration of damaged tissues. Recently, biomaterials that can regulate immune cells especially macrophages have been spotlighted in tissue regeneration. However, the development of multifunctional hydrogel dressings with intrinsic macrophages modulation ability, antioxidant, hemostatic, and antibacterial property for burn wound healing remains challenging and has been rarely reported. Graphene oxide (GO), with its various physicochemical properties, such as biocompatibility, hydrophilicity, and ease of functionalization, has considerable potential in the medical industry for drug delivery and tissue engineering. GO has been shown to enhance the presence of pre-regenerated M2 macrophages effectively and inhibit macrophage cytokine production [10,22,23]. Based on these studies, GO-based composite hydrogels can alter the macrophage phenotype and contribute to diabetic wound healing *in vivo* to activate the immune system.

Redox balance plays a key role in wound healing and skin tissue regeneration. Tissue damage produces excess reactive oxygen species (ROS), prolongs the inflammatory response and leads to oxidative damage to subcellular components, preventing tissue regeneration. Therefore, dynamic modulation of ROS levels is essential for effective wound treatment [24]. TA is a natural polyphenol extracted from plants with a glucose core attached to five phenylenediol groups and five catechol groups. Its abundant phenolic hydroxyl groups can be easily combined with various natural polymers through various interactions (non-covalent and ligand bonds) to form hydrogel systems. TA confers the inherent anti-inflammatory and antioxidant properties of hydrogels, and achieves anti-inflammatory properties by scavenging ROS to accelerate wound repair. In addition, TA also enhances the hemostatic effect of hydrogels through interactions with blood proteins. TA is also the natural antimicrobial agents, which can deprive microorganisms of the essential element [25–27]. In addition, polydopamine (PDA)-modified GO (GA) can effectively interact with bacterial cell membranes. Disruption of the integrity of the cell membrane allows the internal contents of the cell to leak out, which leads to the death of bacteria [28,29]. TA and GA synergistically antibacterial and improved antibacterial efficiency. This combination is considered a promising non-antibiotic strategy.

Mg^{2+} is an abundant transition-metal ion in the human body. An increasing number of studies suggest that Mg^{2+} promotes angiogenesis and plays an important role in the maintenance of homeostasis, immune function, and oxidative stress [30–32]. Gelatin is a hydrolysate of collagen, which has the advantages of biodegradability, good biocompatibility and non-immunogenicity. It is functionally and physically similar to the extracellular matrix (ECM), which provides important advantages as a burn-wound dressing [33–35]. However, gelatin hydrogels with multifunctional properties, such as shape adaptation, biodegradability, hemostasis, anti-inflammatory, and antimicrobial properties, have not been reported as burn-wound dressings.

In this study, we design a gelatin-based PDA-modified GO hydrogel (GTMG) containing TA and Mg^{2+} to modulate immune cells and promote burn-wound healing. The GTMG hydrogel possesses shape-adaptive, biodegradability, effective antimicrobial, hemostatic, antioxidant, and conductive properties. The effects of the hydrogel on macrophage polarization, cell proliferation, migration, and angiogenesis are also investigated. A burn model is used to evaluate the healing effects of the GTMG hydrogel. The results demonstrate that the GTMG hydrogel greatly reduces the burn-healing time and accelerates the reconstruction of skin structure and function. This study suggests that GTMG multifunctional hydrogel has considerable potential for application as a burn-wound dressing.

The results showed that the hydrogel greatly reduced burn healing time and accelerated the reconstruction of skin structure and function.

2. Materials and methods

2.1. Materials

Dopamine (DA), TA and $MgCl_2$ were purchased Sigma-Aldrich. GO was obtained from Nanjing Muke nano-technology Co. Ltd (China). methacrylated gelatin (GelMA, EFL-GM-60) and lithium phenyl-2,4,6-trimethybenzoylphosphinate (LAP) were bought from Suzhou Intelligent Manufacturing Research Institute (China). All other reagents used in the experiments were of analytical grade and did not require further purification.

2.2. Synthesis of GA and hydrogels

100 mg of DA was added to 10 mL of GO solution and sonicated for 20 min at room temperature followed by stirring for 30 min to obtain a GA solution for subsequent experiments.

LAP was dissolved in PBS (pH 7.4) at 55 °C to obtain a LAP solution at a concentration of 0.25 % (w/v). Subsequently, GelMA powder was dissolved in LAP solution at a concentration of 11 % (w/v). Finally, photocrosslinking (Suzhou Institute of Intelligent Manufacturing, Suzhou, China) was performed by dissolving 1 mg of $MgCl_2$, 25 mg of TA, and 55 μL of GA solution in 1 mL of GelMA solution, sonicated for 10 min, and then stirred at 50 °C followed by using a flashlight with visible light (405 nm, 30 mW/cm^2) for 15 s in order to obtain a GTMG hydrogel. The hydrogel of undoped GA solution was GTM.

2.3. Characterization

Scanning electron microscopy (SEM), Mapping, UV–Vis spectrophotometry, FT-IR spectroscopy, were used to examine physical properties of the hydrogels. The mechanical properties of the hydrogels were examined by a dynamic mechanical analyzer TA instrument (DMA Q800).

2.4. Swelling and degradation of the hydrogels

The swelling and degradation of the hydrogels (Gel, GTM and GTMG) were measured with the swelling ratio and residual mass ratio, respectively.

2.5. Adhesive, injectability and shape adaptability of the GTMG hydrogel

The adhesive property of the hydrogels (Gel, GTM and GTMG) was assessed by quantitative and macroscopic qualitative experiments. The tests of injectability of the GTMG hydrogel are described in the supporting information. Preparation of GTMG hydrogel by star-shaped molds to evaluate the shape adaptability.

2.6. Cytocompatibility, migration and tube formation of the hydrogels

Cytocompatibility of the hydrogels was tested by a Live & Dead staining. The cell proliferation was measured by cell counting Kit-8 (CCK-8). The NIH-3T3 cells were used for cell scratch tests to obtain the cell migration ability. The *in vitro* angiogenic effect of hydrogels (Gel, GTM and GTMG) was assessed by the human umbilical vein endothelial (HUVEC) tube formation assay. The detailed procedure was provided in the Supporting Information.

2.7. Antioxidant and antibacterial properties of hydrogels

The antioxidant property of the hydrogel (Gel, GTM and GTMG) was studied by the DPPH method. The cellular ROS scavenging activity was tested by the reactive oxygen species assay kit (2′,7′-dichloro fluorescein diacetate, DCFH-DA). RAW 264.7 cells (3×10^5 cells per well) were cultured with the extract of the hydrogels (Gel, GTM and GTMG) for 12 h, then the ROS levels were measured by CLSM and flow analyzer.

The antibacterial property was investigated by using *S. aureus* and *E. coli* contact with the hydrogels (Gel, GTM and GTMG). The detailed process is provided in Supporting Information.

2.8. Assessment of M2 macrophage-polarized in vitro

To assess hydrogel-induced macrophage polarization, Raw 264.7 was incubated in 6-well plates for 12 h. The medium was replaced with lipopolysaccharide (LPS) or interleukin-4 (IL-4) solution. After 24 h, the above solutions were removed and the collected cells were co-cultured with the hydrogel extracts. The extract of the hydrogel was prepared in complete medium at 37°C for 5 d. Cells treated with fresh medium after LPS or IL-4 served as controls [11].

The cells were then incubated in an incubator for 12 h to allow reattachment. The walled cells were fixed with 4 % paraformaldehyde and blocked with 1 % bovine serum albumin. Then, the cells were incubated with CD206 primary and secondary antibodies and Hoechst 33258 and imaged by CLSM. For flow cytometry, cells were incubated with CD86 and CD206 antibodies.

Concentrations of cytokines (Interleukin-10 (IL-10), interleukin-6 (IL-6) and tumor necrosis factor-α (TNF-α)) in cell culture supernatants were measured using ELISA kits as directed by the manual.

2.9. In vivo hemostasis properties of the hydrogels

All animal experimental procedures were approved by the Ethics Committee of Fourth Military Medical University (approval reference number KY20193145) in full accordance with the ethical guidelines of the National Institutes of Health for the care and use of laboratory animals. The hemostatic properties of GTMG hydrogel *in vivo* were evaluated by using a mouse hemorrhagic liver model.

2.10. In vivo degradation of the hydrogels

In vivo biodegradability of GTMG hydrogels was evaluated by subcutaneous injection. Masson trichrome and hematoxylin-eosin (H&E) stained tissue sections to evaluate the histocompatibility of GTMG hydrogels.

2.11. Evaluation of burn wound healing in vivo

A deep second-degree model was established on the back of Balb/c mice (female, 5–6 weeks old, 30–40 g) using preheated aluminum metal rods to evaluate the therapeutic effect of GTMG hydrogel on burn wounds. GTMG hydrogel (GTMG group) and Urgotul silver sulfadiazine (SSD) dressing (SSD group) were applied to the backs of mice for wound treatment, and the untreated group served as a control group (Con group). Regenerated tissues were evaluated by H&E, Masson trichrome staining, immunohistochemistry and immunofluorescence staining. IL-6, TNF-α, neovascularization (CD31 and α-SMA), collagen deposition, M1 macrophage markers (CD86 and iNOS), VEGF and M2 macrophage markers (CD206 and Arg-1) were observed and quantified. Specific experimental methods are in the Supporting Information.

2.12. Statistical analysis

The analysis data was expressed as mean ± standard deviation. Statistical significance between the results was determined by one-way or two-way ANOVA and Student's t-test. $P < 0.05$ was considered to be statistically significant ($^*P < 0.05$, $^{**}P < 0.01$, $^{***}P < 0.001$, $^{****}P < 0.0001$).

3. Results and discussion

3.1. Design and structural characterization of the GTMG hydrogels

The GTMG-hydrogel production and its application to burn wounds are shown in Scheme 1. The rapid healing of burn wounds was aided by the outstanding antibacterial and antioxidant properties of GTMG and M2 polarization of macrophages. Owing to its redox activity, stability, and binding properties, PDA first reduced GO and polydopamine-functionalized graphene oxide (GA) (Fig. S1). The GTMG multifunctional-hydrogel system was then effectively created by introducing TA, Mg^{2+}, and GA into the interior of GelMA. GelMA is a photosensitive biohydrogel made of gelatin and methacrylic anhydride with excellent biocompatibility. When cured with ultraviolet (UV) or visible light, GelMA forms 3D structures with a degree of intensity that is conducive to cell development and differentiation. As illustrated in Fig. 1D, the photoinitiator LAP was photocrosslinked at 405 nm and 30 mW/cm^2 for 15 s under UV irradiation to form a hydrogel system. The hemostatic process was enhanced by the hydrogel's fast capture of blood cells owing to the reduced gelation period. Fig. 1 shows the typical microstructure and physicochemical properties of the hydrogel. The porous morphology of the hydrogel was observed by scanning electron microscopy (SEM). As shown in Fig. 1A–C, the hydrogel exhibited a clear 3D porous architecture, and the addition of GA gradually increased the average pore size of the hydrogel. This shows that the addition of GA establishes both dynamic hydrogen bonds with GelMA and GA/Mg^{2+} metal-ligand linkages with Mg^{2+} in a competitive manner, reducing the cross-linking density of GelMA/TA, resulting in a looser network of GTMG hydrogels than GTM hydrogels. The porous, loose network structure of the hydrogel dressing simplifies the exchange of gases and nutrients at the wound site while enabling better absorption of tissue exudates [33].

Elemental mapping (Fig. 1E) revealed that the elements C, N, O and Mg were distributed throughout the GTMG hydrogel uniformly. A typical GA absorption peak was observed at 280 nm in the UV-absorption spectrum of GTMG (Fig. 1F), indicating that GA was successfully incorporated into the core of the hydrogel. Fourier transform infrared spectroscopy (FITR) spectra observed near 1659, 1535, and 1334 cm^{-1} revealed typical peaks of GelMA (RNH, R_2NH, and R_3N, respectively; Fig. S2). The FTIR results of GTM and GTMG revealed similar characteristic peaks, indicating that the structure of the gel-dominant material had a disordered conformation in all the hydrogels. Both had a typical broad peak at 3270 cm^{-1}, which suggests that hydrogen bonds were formed between TA and GelMA. The stretching vibrations of the aromatic ester C=O, aromatic C=C, and aromatic C-C groups were observed in the TA spectra at 1698, 1606, and 1532 cm^{-1}, respectively. The structures of GTM and GTMG exhibited the aforementioned TA band as well as the C-H telescoping gelatin vibration at 2957 cm^{-1}. The C=O stretching-vibration band of gelatin at 1659 cm^{-1} was comparable to the C=O group stretching vibration of TA at 1698 cm^{-1} (the stretching vibration of the C=O group in the aromatic ester of TA). It merged with the absorption band (aromatic C=C stretching) at

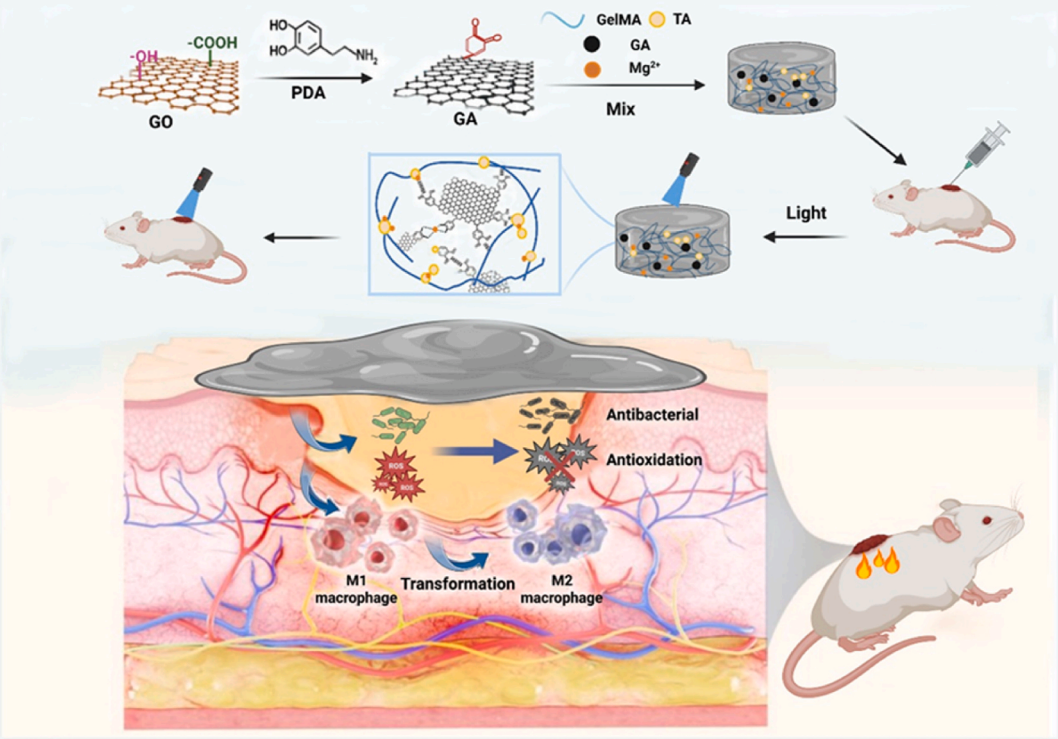

Scheme 1. Schematic illustration of the preparation of the GTMG hydrogel and the multifunctional display of GTMG hydrogel for promoting burn wound healing.

1606 cm^{-1} to form a broad band at 1641 cm^{-1}, demonstrating that TA successfully entered the inner part of the hydrogel system.

3.2. Mechanical property, adhesive, injectable and shape adaptability property of the hydrogels

Rheological tests were performed to assess the mechanical characteristics of the hydrogels under various conditions. For a frequency range between 0.1 and 100 rad/s, the storage module (G′) of the hydrogel greatly outweighed the loss module (G″), thereby validating the elastic behavior and superior mechanical qualities of the hydrogels (Fig. 1G). The two curves in Fig. 1H intersect at a tension of 750 %. The collapse of the GTMG hydrogel structure and the transition from a solid state with gel characteristics to a liquid state with liquid characteristics are manifested by a sharp decrease in the G′ value and an abrupt increase in the G″ value [36].

The addition of GA reduced the Yang's modulus of the hydrogel (Fig. S3A), indicating that GTMG was more flexible and suitable for filling burn surfaces. In addition, the GTMG hydrogel exhibited a shear-thinning ability. The GTMG precursor solution was filled into a star-shaped model with a needle and solidified into a star hydrogel under UV irradiation (Fig. 1J). The viscosity of the GTMG hydrogel steadily decreased with increasing shear rate (Fig. 1I), demonstrating a shear-thinning capability, which was the main contributing factor to injectability. To demonstrate the injectability, the GTMG hydrogel was drawn from the needle's tip and continually formed the letters "AFMU" (Fig. S4). Injectable hydrogels are morphologically adaptable and can be flexibly injected according to the uneven shape of burn wound, and have great potential in the treatment of facial burns due to the larger and more irregular wound shape of burns than other wounds [37].

In contrast, the adhesive hydrogel can adhere to the tissue completely and fuse with it. This not only prevents infection but also makes it suitable for dynamic wounds with high-frequency movement. The GTM and GTMG hydrogels exhibited stronger adhesion to the tissue surfaces (Fig. S3B). The adhesive properties of the hydrogels were further evaluated using the tissue adhesion (Fig. S5). The GTMG hydrogel adhered to major organs, including the heart, liver, kidney, spleen, and lung, without falling under the influence of gravity.

The GTMG hydrogel firmly adhered to freely twisted pigskin and a freely bent elbow joint (Fig. 1K), indicating its good adhesion properties. The hydrogel may be used to establish a stable connection between the burn wound and dressing for various dynamic burn wounds. The main reasons for the high adhesion of hydrogels are as follows: First, inspired by the strong adhesion of mussels, the introduction of catechol groups into hydrogels can enhance adhesion and further improve adhesion strength [38]. Second, the good adhesion of the hydrogels to tissues was mainly attributed to the interaction between the hydrogels and tissues (Fig. 1L). The catechol moiety formed strong covalent bonds with different nucleophilic reagents, such as imidazole, thiols, and amines, as well as hydrogen bonds [39]. The adhesion strength of the GTMG hydrogel makes it a promising candidate for application to dynamic burn wounds, even in organ tissues with frequent movement, such as joints.

Healthcare professionals must change dressings frequently for patients during the process of wound healing, which often causes secondary damage to the wound and prolongs healing time. Therefore, hydrogel dressings with degradation ability appear to be better choices for treating burn wounds [40]. Then the swelling property and degradability of hydrogels were evaluated (Fig. S3C). The good swelling properties of hydrogels facilitated the absorption of wound exudate, thereby accelerating wound repair. Over time, we observed that the hydrogel could be degraded slowly by absorbing water, thus avoiding secondary damage to the wound during dressing changes (Fig. S3D). These results indicate that GTMG hydrogel has good swelling and degradation properties, which is conducive to its application in wound and tissue regeneration.

3.3. Cytocompatibility of the hydrogels

Good cytocompatibility is the most essential property of biomaterials and plays an important role in biomaterial research [41]. CCK-8 experiments showed that compared with the Con group, the proliferation

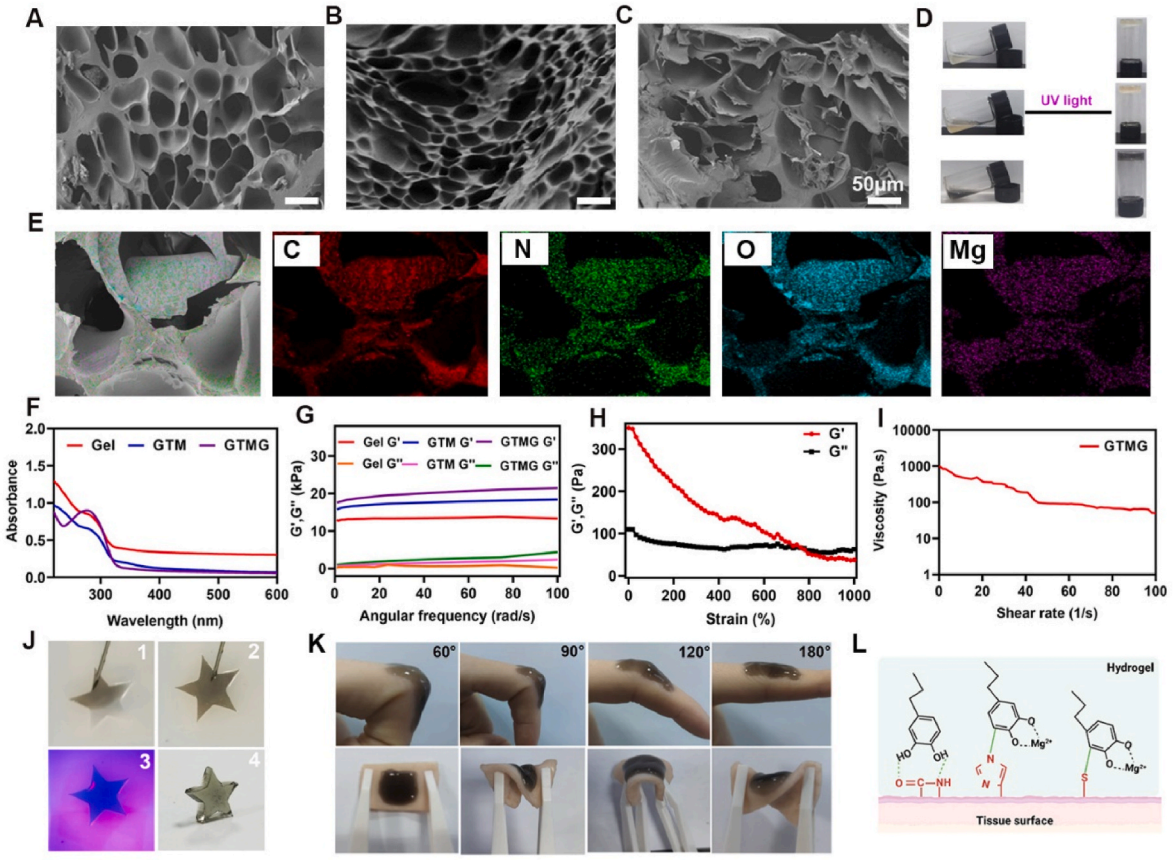

Fig. 1. Characterization of hydrogels. (A–C) SEM images of the Gel, GTM and GTMG. (D) Macroscopic observation of the hydrogels formation through photo-crosslinking. (E) Distribution of elements (C, N, O, Mg) of the GTMG. (F) UV–vis spectra of Gel, GTM, and GTMG hydrogels. (G) G′ and G″of the hydrogels (Gel, GTM, and GTMG) under angular frequency sweep. (H) G′ and G″of the GTMG hydrogel under strain amplitude sweep. (I) Shear thinning properties of the GTMG hydrogel. (J) The injectability and photocuring of GTMG hydrogel. (K) Adhesion effect of the GTMG hydrogel on human elbow and porcine skin during exercise. (L) The adhesive mechanism of the GTMG hydrogel. (*$P < 0.05$, **$P < 0.01$, ***$P < 0.001$, ****$P < 0.0001$, ns: no significant difference).

of NIH-3T3 cells in all hydrogel groups showed a significant increase trend within 3 days, indicating that the hydrogel groups had good biocompatibility and non-toxicity (Fig. 2A and D). Live/dead cell staining further confirmed the impact of the hydrogel on cell viability (Fig. 2A). All experimental groups showed normal cell growth and high expression of green fluorescence, with few dead cells after hydrogel administration.

3.4. Effectiveness of hydrogels in promoting cell migration and tube formation in vitro

Previous studies have shown that enhanced cell migration accelerates wound healing [42]. The effect of cell migration was assessed using an *in vitro* wound-healing scratch assay in which a straight line was drawn into a confluent NIH-3T3 cell monolayer to create an artificial wound that filled the gap by facilitating cell migration.

After 24 h of co-incubation with cells, all hydrogel groups showed higher cell migration efficiency than the Con group (Fig. 2B and E). The main reason is that gelatin is a hydrolysate of collagen that promotes cell adhesion and migration. After culturing the cells for 24 h, the GTM and GTMG groups exhibited higher migration rates than the Gel group. There are two main reasons: first, cells co-cultured with hydrogels with higher elastic modulus and stronger adhesion exhibit faster migration [43,44]; second, Mg^{2+} stimulates cell migration and proliferation to promote angiogenesis and accelerate wound closure [30–32].

The angiogenic ability of the GTMG hydrogel was further evaluated by performing an *in vitro* angiogenesis assay. The results showed that angiogenesis of HUVEC cells in the GTM and GTMG groups was significantly increased compared with that in the Con group, and the branch point and mean tube length were significantly increased (Fig. 2C and F). In summary, we successfully verified the ability of the GTMG hydrogel to promote cell migration and angiogenesis *in vitro*, laying a good foundation for its ability to promote wound healing *in vivo*.

3.5. Antioxidative properties

Antioxidant, conductive, and antimicrobial properties are important bioactive multifunctional properties. High levels of ROS severely impede tissue regeneration, which is one of the main reasons why burn wounds are difficult to heal [45]. A 1,1-diphenyl-2-picrylhydrazyl (DPPH) free-radical scavenging assay was used to evaluate the antioxidant activity of the hydrogels [33,34]. The Gel solution was purple in color and had little antioxidant capacity, whereas the solution of the GTMG and ascorbic acid groups was light yellow, indicating that the GTMG hydrogel was effective in scavenging free radicals with an antioxidant efficiency of up to 90 % (Fig. 3A and B). However, in the Gel group, the DPPH scavenging rate was only 8 %, owing to the absence of catechol groups. The main reason for the excellent antioxidant activity of the GTMG hydrogels is the presence of catechol groups in TA and GA. The catechol groups present in TA and GA directly scavenge ROS and reduce inflammation through reduction reactions.

Excellent antioxidant properties protect cells from ROS-induced damage. The level of intracellular ROS scavenging by the GTMG hydrogel was assessed using the DCFH-DA probe. The fluorescence intensity of the hydrogel after co-culture with RAW 264.7 cells could determine the level of intracellular ROS; the Gel group exhibited

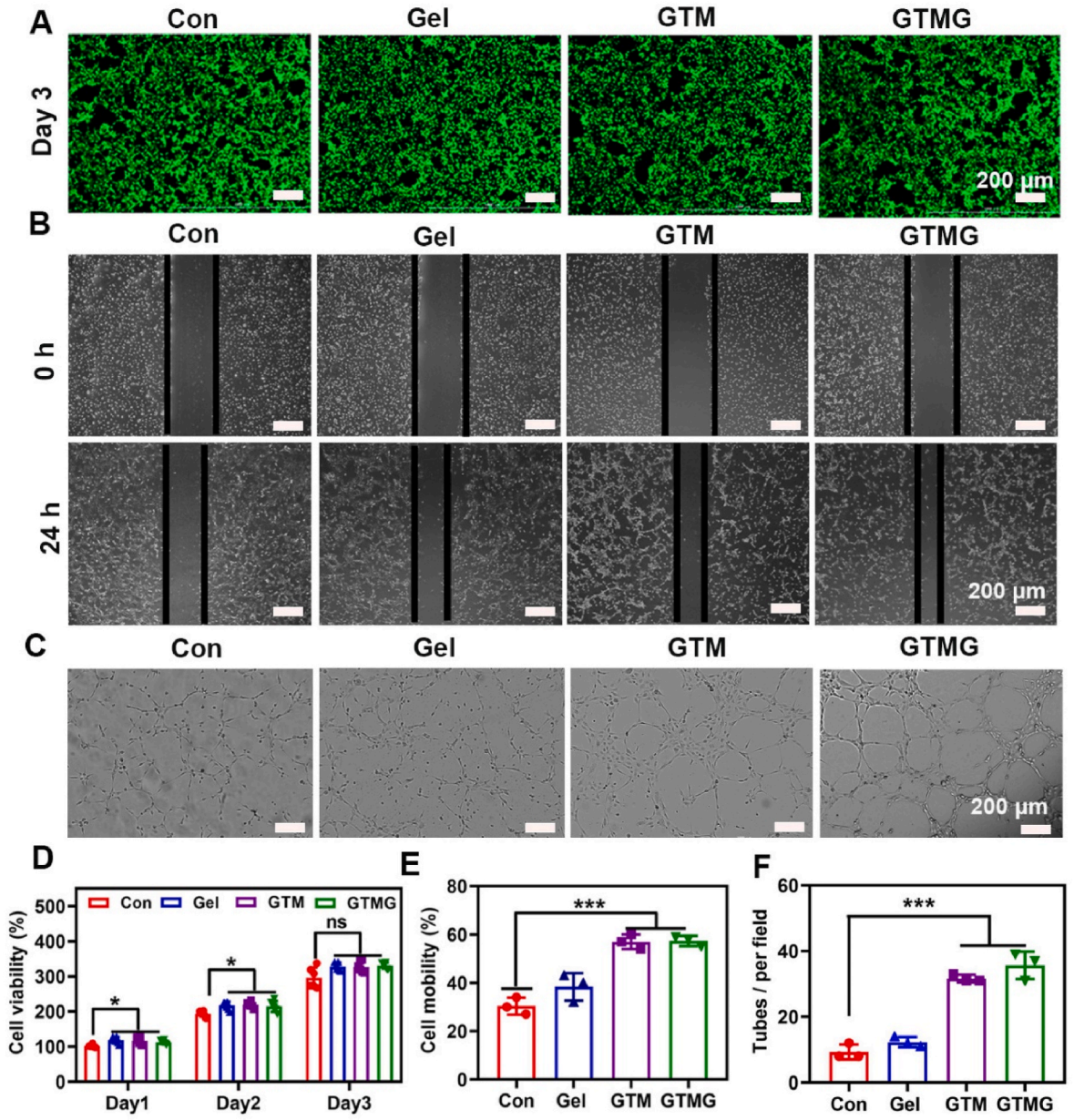

Fig. 2. Cytotoxicity, cell migration and tube formation of the hydrogels. (A) Live/dead staining of NIH-3T3 cells. (B) Cell migration of NIH-3T3 cells. (C) Images of tube formation by HUVECs. (D) Cell viability (n = 6) and (E) cell mobility (n = 3) of the hydrogels. (F) The number of tubes per field of the hydrogels (n = 3). (*P < 0.05, **P < 0.01, ***P < 0.001, ****P < 0.0001, ns: no significant difference).

stronger fluorescence intensity, whereas the GTMG hydrogel had the lowest fluorescence intensity (Fig. 3D). Flow cytometry was used to confirm the intracellular antioxidant activity. The ROS-positive rate of the GTMG hydrogel was 14.44 %, which was similar to that of the negative control group (Fig. 3E). These results showed that the GTMG hydrogel effectively prevented cell damage caused by excessive ROS under oxidative stress. The electrical conductivity of the GTMG hydrogel was significantly higher than that of the other groups, which was mainly owing to the good electrical conductivity of GA (Fig. S6A). Therefore, GTMG hydrogel can be combined with electrical stimulation for the treatment of burn wounds [10].

3.6. Antibacterial capability of the hydrogels

Burn wounds produce more exudates than other wounds and have a higher risk of bacterial infection, which leads to delayed healing. The inherent antimicrobial properties of hydrogel dressings protect the wounds from external bacterial infections and remove bacteria from the wound site. We tested the antimicrobial ability of the GTMG hydrogels not only *in vitro* against Escherichia coli (*E. coli*, a gram-negative bacterium) and Staphylococcus aureus (*S. aureus*, a gram-positive bacterium) but also *in vivo* against *E.coli* (Fig. 3C, Fig. S6B-C and S7). The antimicrobial properties of the GTM and GTMG hydrogels were significantly better than those of Gel hydrogels. Considering the potential antibacterial ability, the addition of TA destabilized the microbial cytoplasmic membrane, increased membrane permeability, and interacted with bacterial proteins to produce enzyme inhibition. In addition, the hydroxyl group of TA reacted with the sulfhydryl group (-SH) in the pathogen protein to destroy its structure, ultimately leading to the loss of its proliferative ability [46,47].

The above results indicated the excellent antibacterial capability of the GTMG hydrogel *in vivo* and *in vitro*. Due to the synergistic antimicrobial activity of TA and GA, the antimicrobial activity of GTMG hydrogels was better than that of GTM hydrogels. GA can not only

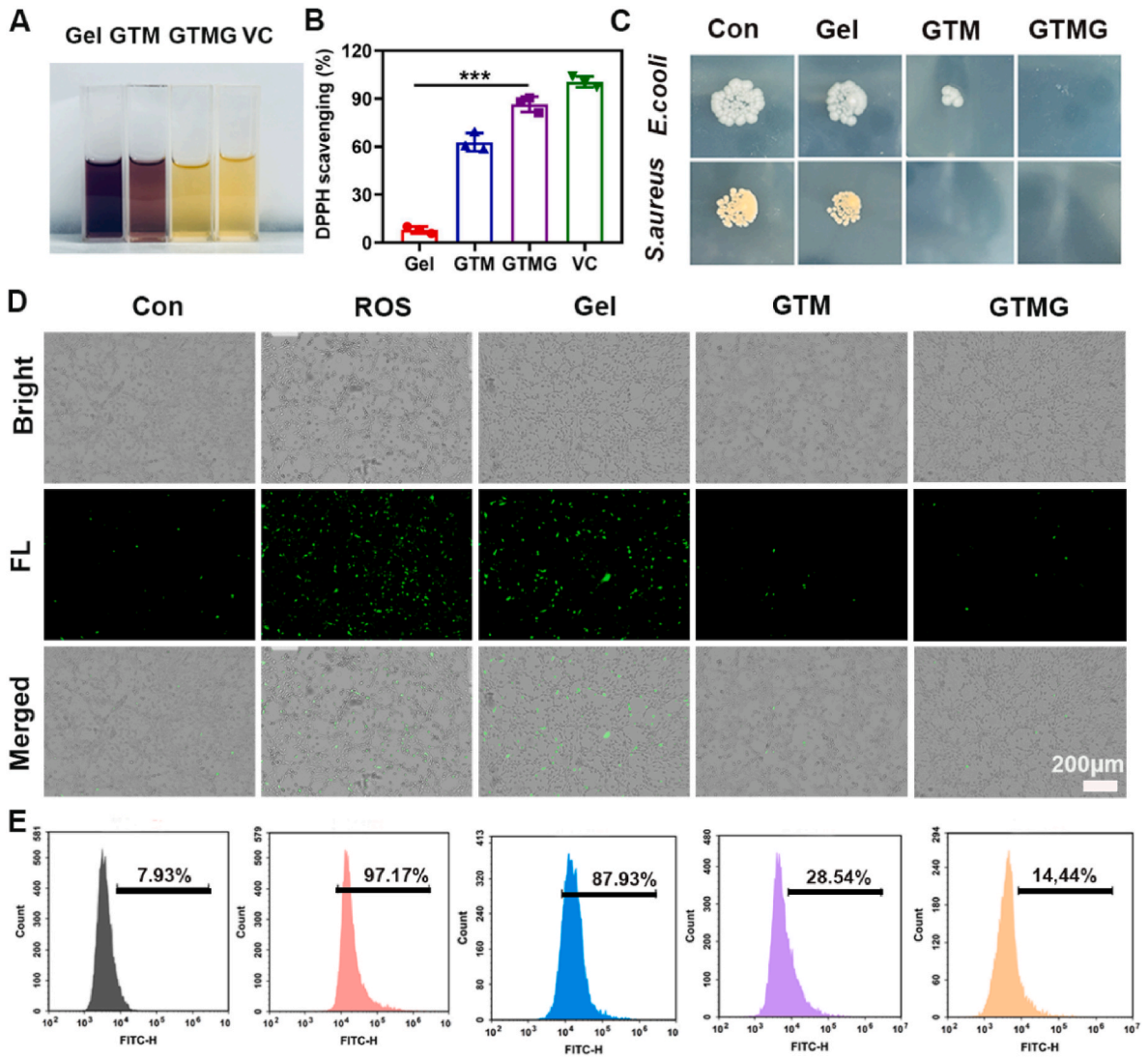

Fig. 3. Antioxidative and antibacterial property of the hydrogels *in vitro*. (A) Optical photograph of the color change and (B) DPPH-scavenging efficiency of Gel, GTM, GTMG hydrogels and VC. (C) Images of survival bacterial (*S. aureus* and *E. coli*) CFUs on agar plates after contact with various hydrogels. (D) Intracellular ROS-scavenging performance of different hydrogels (Gel, GTM and GTMG). (E) Flow cytometric analysis of 2′,7′-dichloro fluorescein diacetate (DCFH-DA)-labeled cells on the Gel, GTM and GTMG hydrogels. (the data are presented as the mean ± SD (n = 3), $^{*}P < 0.05$, $^{**}P < 0.01$, $^{***}P < 0.001$, $^{****}P < 0.0001$, ns: no significant difference). (For interpretation of the references to color in this figure legend, the reader is referred to the Web version of this article.)

disrupt the bacterial membrane structure, but also interact with bacteria to cover the bacterial surface, isolate the bacteria from the external environment and block their active sites. This led to a significant decrease in bacterial bioactivity, which helped TA further capture the surrounding bacterial cells. In addition, the antibacterial activity of GTMG was more effective against *S. aureus* than *E. coli* owing to the different cell-wall compositions and structures of *S. aureus* and *E. coli* (Fig. 3C). The cellular affinity of the catechol moiety enabled the GTMG hydrogel to exhibit excellent antibacterial activity, while maintaining good cytocompatibility.

3.7. Immunomodulatory activity of the GTMG hydrogel in vitro

Persistent inflammation is one of the most prominent features of burn wounds, and the transition from the inflammatory to the proliferative phase is a key regulatory point for wound healing. Hydrogel dressings with functional properties that modulate inflammation are required to effectively promote wound healing. M1 macrophages secrete pro-inflammatory mediators when they receive stress-factor signals, whereas M2 macrophages secrete anti-inflammatory cytokines and therapeutic growth factors when they receive immune signals. However, the burn-tissue microenvironment prevents the phenotypic shift of macrophages from the pro-inflammatory (M1) to anti-inflammatory (M2) phase, resulting in chronic inflammation and delayed wound healing. RAW 264.7 macrophages were co-cultured with the hydrogels to explore the regulatory effects of GTMG hydrogel on macrophages. LPS and IL-4 were used to produce M1 and M2 phenotypes in macrophages, respectively, as previously reported [19]. Immunofluorescence staining with CD206 (a marker for M2 macrophages) was used to assess the transformation and maintenance of the M1 and M2 phenotypes after the hydrogel treatment. Compared with the IL-4 control group (0 h), the relative expression level of CD206 was significantly lower in the IL-4 control group (72 h) without the hydrogel (Fig. 4A and S8A). However, no significant difference in the relative expression levels of CD206 and IL-4 (0 h) was observed after 72 h of the GTMG hydrogel treatment, suggesting that the GTMG hydrogel maintained the M2 phenotype of macrophages. The relative expression levels of CD206 were almost absent in the LPS control group (0 h) (Fig. S8B). The results demonstrated that GTMG hydrogel can effectively activate macrophage polarization to M2 phenotype.

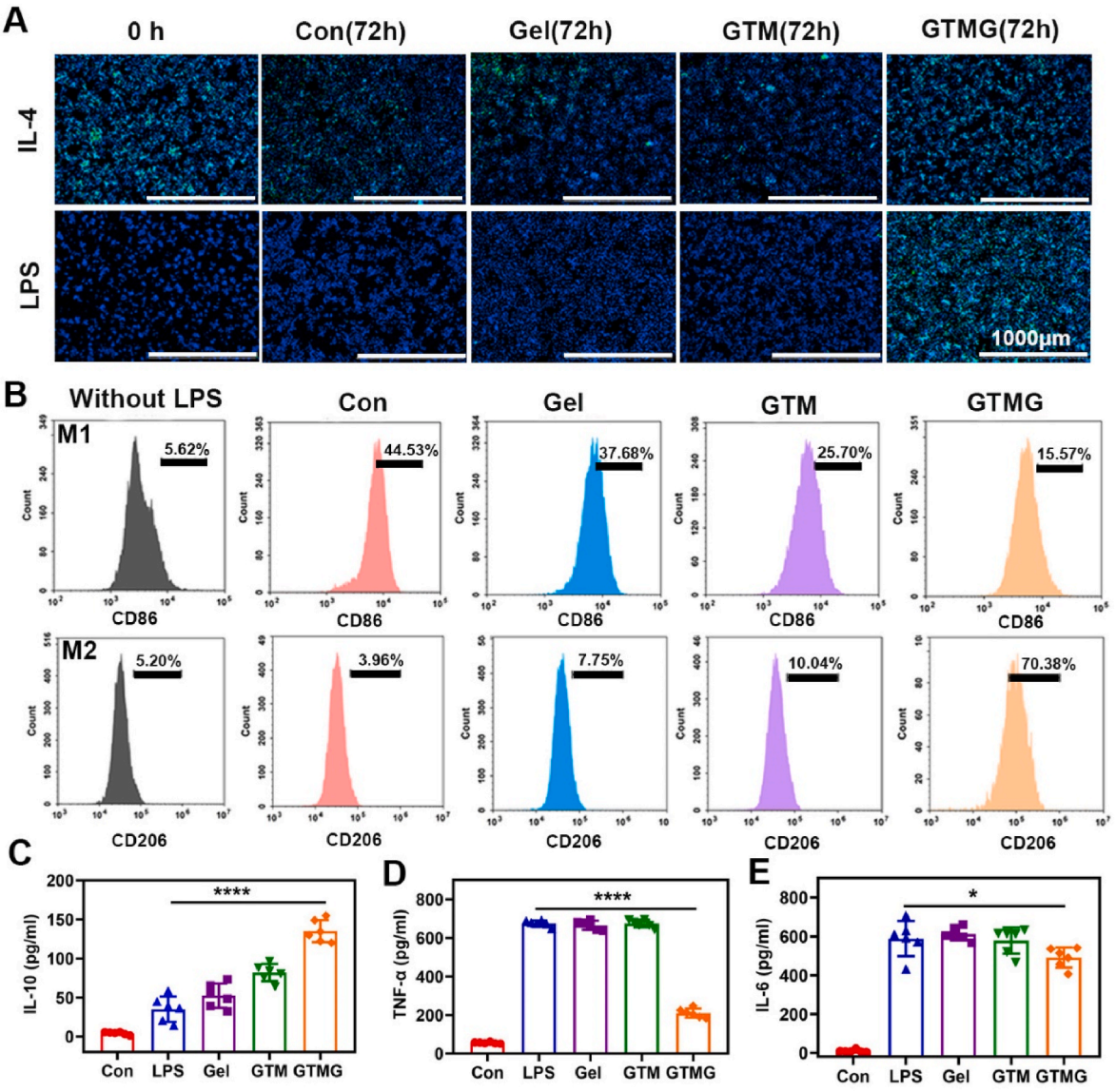

Fig. 4. Immunomodulatory property of the hydrogels *in vitro*. (A) Photographs of RAW 264.7 stained with CD206 after cultured with different hydrogels (Gel, GTM, GTMG). (B) Polarization of macrophages was evaluated by expression of CD86 (M1) and CD206 (M2) using flow cytometry. ELISA assay of (C) IL-10, (D) TNF-α, and (E) IL-6 in cell culture supernatants. (the data are presented as the mean ± SD (n = 6), $^{*}P < 0.05$, $^{**}P < 0.01$, $^{***}P < 0.001$, $^{****}P < 0.0001$, ns: no significant difference).

We selected CD86 (a marker for M1 macrophages) and CD206-positive cells to test macrophage polarization using flow cytometry to further demonstrate the effectiveness of the GTMG hydrogel in polarizing the macrophage phenotype. RAW 246.7 cells were converted to the M1 phenotype after LPS stimulation. The polarization of M1 macrophages decreased, and the proportion of M2 macrophages increased in the GTMG hydrogel group (Fig. 4B). Previous studies have shown that GO activates polarization of M2 macrophages and promotes angiogenesis [22,23]. The results of Fig. 4B showed that under the stimulation of GTMG hydrogel, macrophages had significantly higher CD206 positive staining levels than other groups, confirming that the polarization state of macrophages was related to the M2 phenotype. At the same time, the expression of M1 and M2 biomarkers was consistent with the results in Fig. 4A, which indicates that the GTMG hydrogel successfully stimulated M2 macrophages and inhibited M1 phenotype. The above results strongly demonstrate the ability of GTMG hydrogel to promote M2 phenotype polarization of macrophages *in vitro*, which should be mainly induced by the GO and GA components of the hydrogel. According to reports, GA has abundant carboxyl and hydroxyl groups, which can interact with growth factors or other proteins through covalent, electrostatic, and hydrogen bonds, thereby affecting cell reactions while promoting cell differentiation and inducing macrophages from M1 to M2 phenotype [22,23]. Therefore, chemical clues and binding interactions with GA are highly likely to lead to M2 polarization of macrophages. Together with the above results, it can be inferred that the GTMG hydrogel effectively stimulated macrophages polarized into M2 phenotype and increased the proliferation and migration of cells involved with healing through the paracrine pathway from M2 macrophages. However, whether the GTMG hydrogel stimulated M2 polarization functions in burn wounds remains unclear.

An enzyme-linked immunosorbent assay showed that the proinflammatory mediators (IL-6 and TNF-α) secreted by M1 macrophages in the GTMG hydrogel group were effectively suppressed compared with the Con group (Fig. 4D and E). In contrast, the anti-inflammatory factor IL-10 was significantly increased (Fig. 4C). These results indicated that GTMG could reduce the production of inflammatory cytokines and accelerate burn-wound repair by regulating the microenvironment of the wound tissue.

3.8. Hemostatic performance of the hydrogels

Massive bleeding from the skin occurs in burns, and the hemostatic phase is the initial stage of wound healing [39]. Excellent hemostatic capability is essential for hydrogel dressings. We established a hepatic hemorrhage model to evaluate the hemostatic ability of the GTMG hydrogel (Fig. 5A). After injecting the hydrogel solution into the wound, the solution rapidly gelled with blood in situ under UV irradiation and hemostasis was achieved as it adhered to the wound surface. Almost no bleeding was observed in the GTMG hydrogel group, which greatly reduced the bleeding volume and shortened the bleeding time (Fig. 5C–E). The excellent hemostatic performance of the GTMG hydrogel was attributed to the synergistic effects of its bioadhesive and procoagulant activities. Rapid gelation of the hydrogel accelerated the capture of blood cells, and the strong adhesion of the GTMG hydrogel tightly adhered to the bleeding site, serving as a physical barrier to facilitate the hemostatic process. Gelatin can also provide arginine-glycine-aspartic acid peptide sequences, which can lead to good cell adhesion and higher hemostatic capacity for GTMG. In addition, TA can bind to proteins on cell membranes through strong hydrogen bonding and hydrophobic interactions, and catechol groups can enhance the adhesion and activation of blood cells and improve their clotting ability. Hemocompatibility plays an important role in the study of biological materials. The hemolysis test showed that none of the blood cells ruptured upon contact with the hydrogel (Fig. 5B), proving its good blood compatibility [48,49].

3.9. Biodegradability study of the GTMG hydrogel

The advantage of innovative hydrogel dressings is their ability to degrade during wound healing. Based on *in vitro* studies, the hydrogel was fully destroyed on day 13 ((Fig. S3D). Next, the reaction between the hydrogel and tissue was observed by the subcutaneous injection of the GTMG hydrogel prepolymer to evaluate the histocompatibility and biodegradability of the hydrogels. The volume of both the hydrogels decreased considerably over time, with moderate degradation on day 3, significant degradation after day 6, and complete hydrogel destruction by day 15 (Fig. 5F and G).

No significant signs of tissue necrosis, swelling, or hemorrhage were observed in the subcutaneous-implantation areas of the hydrogels. The inflammatory response of the tissues was characterized by H&E and Masson staining. H&E and Masson staining of the tissues on days 1, 4, 7, 10, and 13 showed almost no inflammatory cells (Fig. 5H), indicating that the degradation products of the hydrogel did not exacerbate the

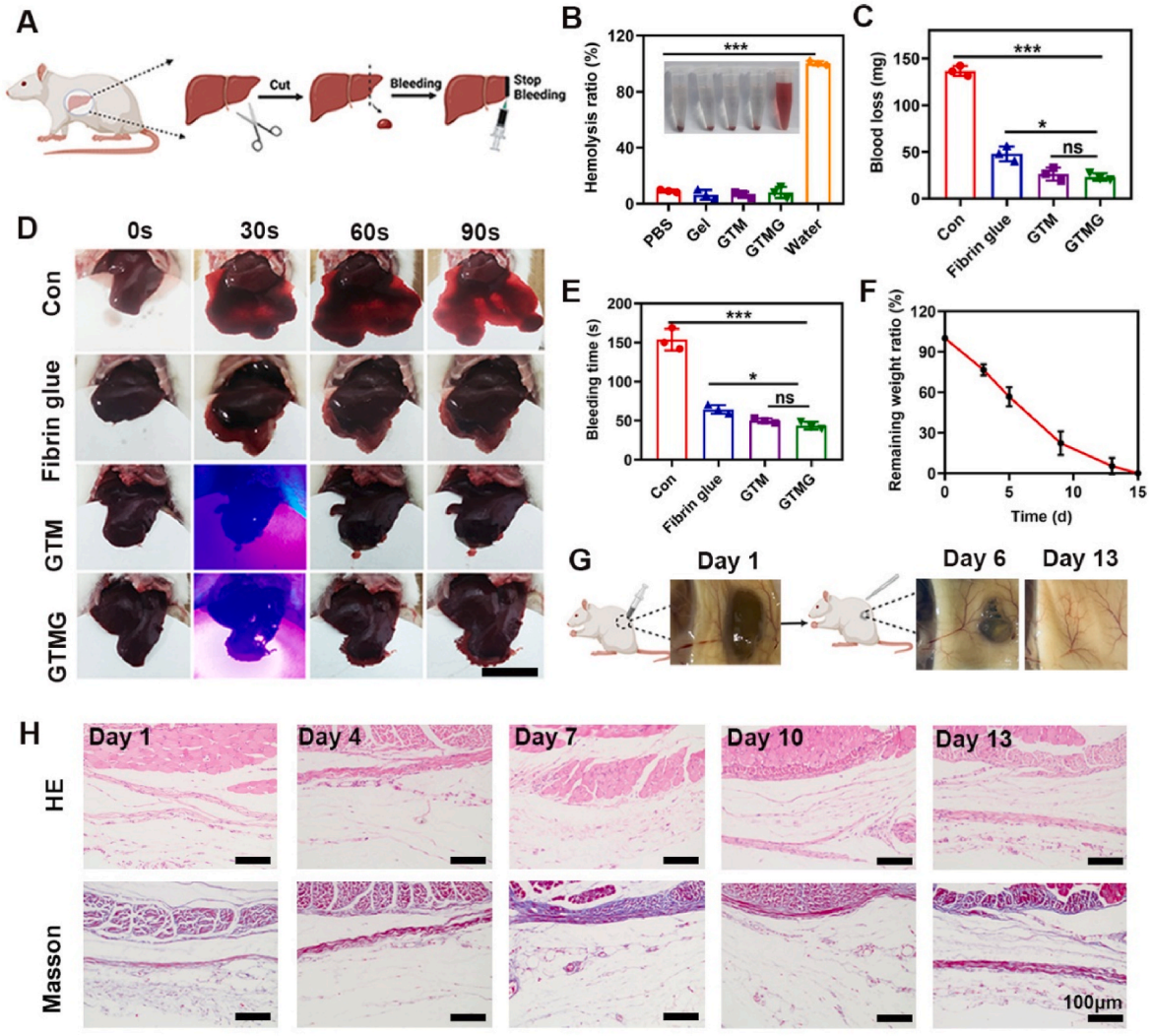

Fig. 5. Hemostatic properties and degradability of the GTMG hydrogel. (A) Schematic illustration of the hydrogel hemostasis process; (B) The hemolytic activity of hydrogels; (C) Bleeding loss in various groups. (D) Photograph of hemostasis process (Scale bar = 1 cm). (E) Blood time in various groups. (F) Degradation time curve of hydrogels *in vivo*. (G) The photographs of GTMG hydrogel *in vivo* on day 1, 6, and 13. (H) Hematoxylin-eosin staining and Masson's trichrome of the tissues around the injection sites. (the data are presented as the mean ± SD (n = 3), $^{*}P < 0.05$, $^{**}P < 0.01$, $^{***}P < 0.001$, $^{****}P < 0.0001$, ns: no significant difference).

inflammatory response. In conclusion, the *in vitro* and *in vivo* studies demonstrated that the GTMG hydrogel had good biocompatibility and *in vivo* degradability, laying a safe foundation for further *in vivo* studies.

3.10. In vivo wound healing efficacy study

In vitro studies demonstrated that GTMG hydrogels have various excellent bioefficacies, including antimicrobial, hemostatic, tissue-adhesion, and shape-adaptation properties. Therefore, GTMG hydrogel is expected to be a promising dressing for the treatment of burn wounds. We evaluated the efficacy of the GTMG hydrogel using a burn-wound model (Fig. 6A), where Urgotul silver sulfadiazine (SSD) dressings were set as the commercial group and untreated wounds were set as the blank control group (Con). The therapeutic efficacies of the Con, SSD, and GTMG groups were assessed by observation and tissue collection on days 0, 5, 10, and 15. Macroscopically, the SSD and GTMG hydrogels exhibited faster wound healing than the Con group (Fig. 6B). On day 5, the GTMG group had a smaller wound area than the Con and SSD groups, and its superior anti-inflammatory properties reduced inflammation. On day 10, the GTMG hydrogel-treatment group showed a 95 % wound-healing rate, and the Con and SSD treatment groups also showed a significant tendency to shrink their wounds. On day 15, the wound-healing rate was more than 80 % in both the Con and SSD groups, whereas the wound in the GTMG group was completely healed (Fig. S9).

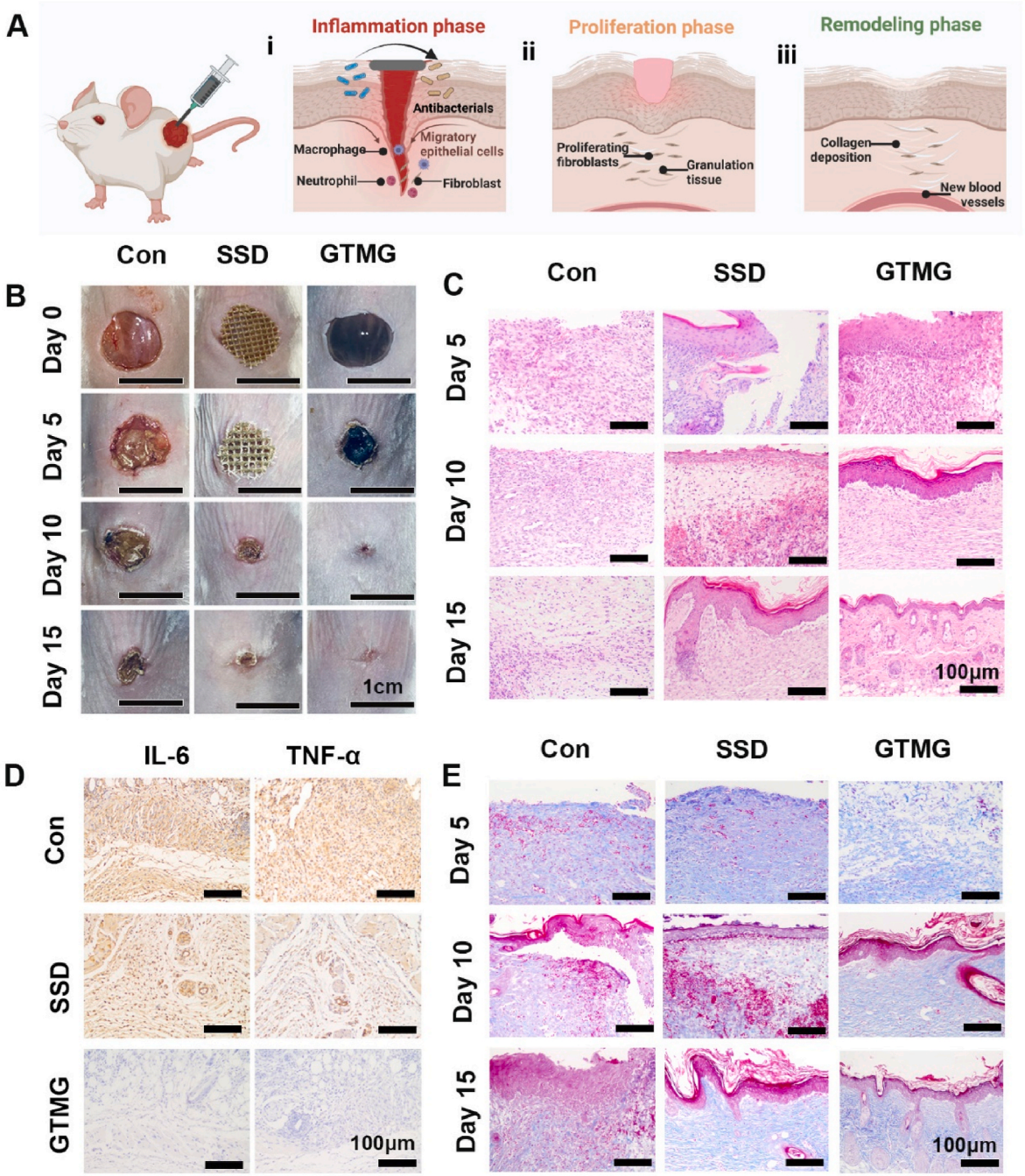

Fig. 6. Treatment efficiency of the burn wound. (A) Schematic illustrations of the burn wound healing process and treatment. (B) Photographs of burn wounds healing with different treatment methods on days 0, 5, 10 and 15. (C) Histomorphological evaluation of different groups. (D) Immunostaining of TNF-α and IL-6 on day 5. (E) Masson staining of wound tissues on days 5, 10 and 15.

These results showed that the GTMG hydrogel accelerated burn-wound healing.

3.11. Histological examination and pro-inflammatory cytokine expression in skin-tissue regeneration

H&E staining was performed to further examine the therapeutic role of the GTMG hydrogel in wound healing from a histological perspective (Fig. 6C). Owing to the anti-inflammatory properties of the GTMG hydrogel, inflammatory-cell infiltration rarely occurred in the initial stages of wound healing. In addition, the hemostatic properties of the GTMG hydrogel permitted the early activation of the inflammatory phase. On day 10, the GTMG and SSD groups showed rapid wound contraction, and the neoepithelialization stage was first observed, whereas the Con group was in the epithelial regeneration stage. This finding indicated that the remodeling phase of the GTMG hydrogel started earlier and accelerated the rate of re-epithelialization by promoting proliferation and migration of fibroblasts, which facilitated the wound-healing process. On day 15, the GTMG hydrogel group showed a higher percentage of neovascularization and hair follicles and healed more completely than the Con and SSD groups. In addition, the human epidermis has a natural endogenous "battery" that generates a small electric current when injured, and wound healing stops when the current is disturbed; so the conductivity of GA might contribute to the skin tissue regeneration via transmitting electrical signals between wound sites and stimulating excitable skin cells. Masson staining revealed that the GTMG hydrogel-treated group had the thickest wound-granulation tissue on day 10 (Fig. 6E). In summary, the multifunctional GTMG hydrogel has considerable potential for the treatment of burn wounds because it can promote skin-structure repair more efficiently than the other groups.

Wound healing is a modular process involving three overlapping but distinct phases: inflammation, proliferation, and remodeling [50]. Next, we evaluated the effects of the GTMG hydrogel on different stages of tissue repair. Pro-inflammatory cytokines such as IL-6 and TNF-α are strongly associated with the recovery of the inflammatory response in the initial phase (Fig. 6D). Immunohistochemistry was used to assess the therapeutic effect of GTMG hydrogel during the inflammatory stage.

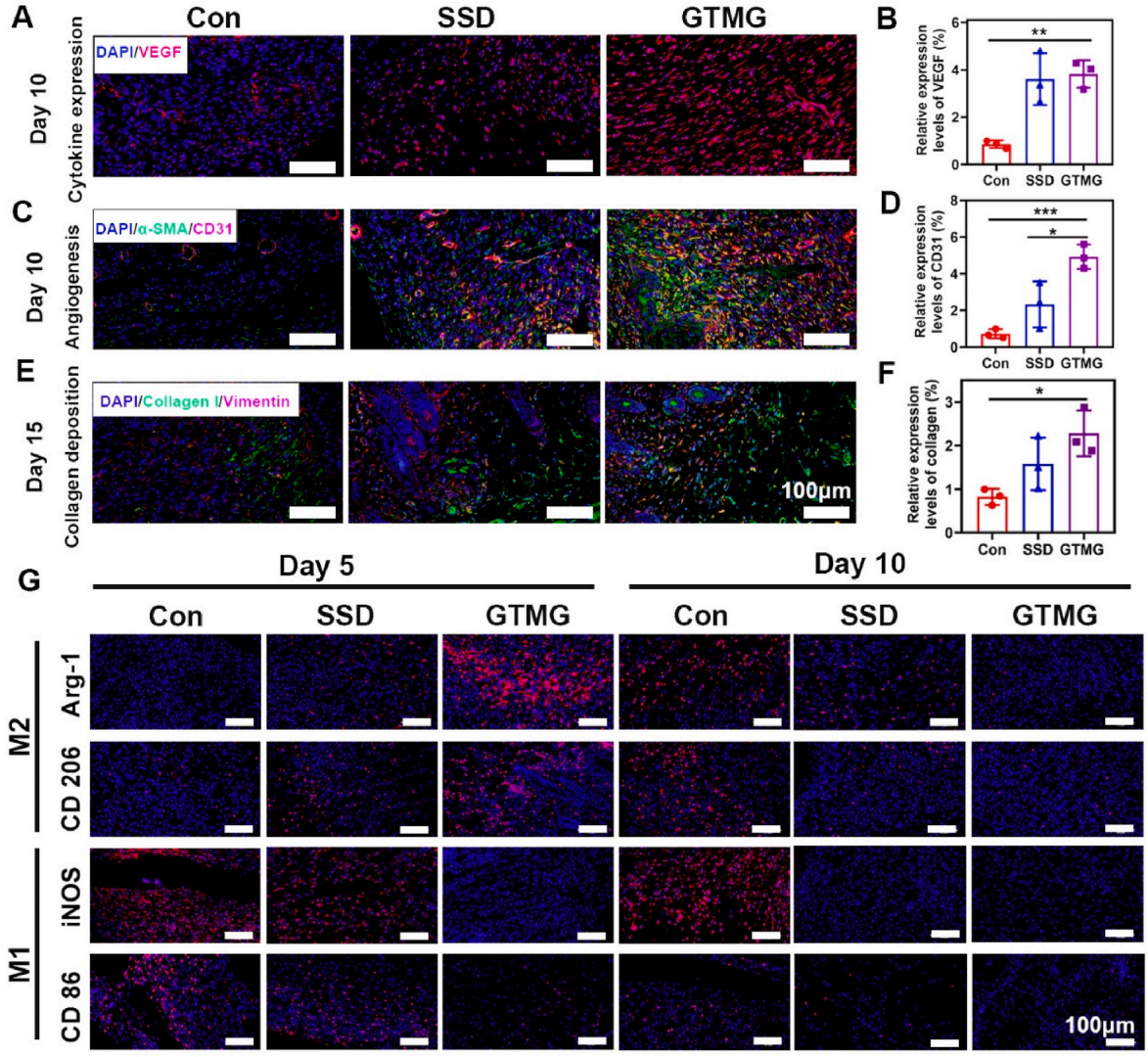

Fig. 7. The biological functional assay of GTMG hydrogel *in vivo*. (A) Representative images and (B) quantified analysis of VEGF (red) on day 10. (C) Representative images of CD31 structures (red) and α-SMA positive cells (green). (D) Quantified analysis of CD31. (E) Representative images of collagen I (green) and fibroblast marker vimentin (red). (F) Quantified analysis of collagen; (For all data, the control group was set as 100 %). (G) Immunofluorescence staining of tissue sections of wound area for CD86 and iNOS (M1-like), CD206 and Arg-1 (M2-like) at day 5 and 10. (the data are presented as the mean ± SD (n = 3), $^{*}P < 0.05$, $^{**}P < 0.01$, $^{***}P < 0.001$, $^{****}P < 0.0001$, ns: no significant difference). (For interpretation of the references to color in this figure legend, the reader is referred to the Web version of this article.)

Compared with the Con and SSD groups, the GTMG group showed the lowest expression of pro-inflammatory factors (IL-6, TNF-α) in the wound area, which accelerated the transition from the anti-inflammatory phase to the proliferative phase [51]. Inflammatory cells continued to infiltrate and displayed a strong inflammatory response in the Con group. The results showed that GTMG hydrogel shortened the duration of the inflammatory phase and accelerated wound healing.

3.12. Study on hydrogels promoting neovascularization and collagen-deposition in regenerated skin tissue

During the proliferative phase, the formation of new blood vessels is essential for maintaining fibroblast proliferation, collagen synthesis, and dermal regeneration [33]. Burns cause more blood loss than other wounds. Therefore, VEGF immunostaining was used to evaluate the impact of the hydrogel on angiogenesis *in vivo*. The GTMG hydrogel group displayed the highest VEGF expression on day 10 (Fig. 7A and B and S10). α-SMA (vascular smooth muscle cell marker) and CD31 (vascular endothelial specific marker) immunofluorescence staining was used to assess neointimal formation. The GTMG hydrogel group showed the highest CD31 expression compared to the Con and SSD groups (Fig. 7C–D and S11). The main reasons for this are as follows: the addition of Mg^{2+} induced angiogenesis and GA-polarized M2-phenotype macrophages, which accelerated neovascularization. Therefore, GTMG hydrogels can effectively promote angiogenesis and the 3D assembly of vascular networks, accelerate the process of epithelial remodeling, and achieve burn-wound healing.

The remodeling phase is the third stage of wound healing, in which more fibroblasts promote the synthesis of a stable ECM that produces a denser collagen reticular skeleton [52]. Double immunofluorescence staining was performed to assess the effect of collagen deposition. Vimentin is the hallmark of fibroblasts, while collagen I is the main component of the skin. During the remodeling phase, the proportion of collagen I in the skin increases. Compared with the Con and SSD groups, the GTMG hydrogel group produced more vimentin and type I collagen deposits, generating a denser collagen reticular skeleton (Fig. 7E–F and Fig. S12). These results suggest that the gelatin skeleton in GTMG hydrogel can promote the migration and proliferation of fibroblasts, as well as collagen deposition and burn wound healing.

3.13. In vivo immune activation of the GTMG hydrogel

Combined with the *in vitro* results of GTMG hydrogel stimulation of M2 macrophage polarization, we further investigated whether reduced inflammation and improved healing were associated with the polarization status of macrophages in burn wounds. On days 5 and 10, M1 (CD86 and iNOS) and M2 macrophages (CD206 and Arg-1) were stained with immunofluorescence to further examine the phenotypic alterations in burn wounds macrophages *in vivo*. The results showed that the GTMG hydrogel group had the highest expression of M2-type macrophages, which effectively reversed the M1-type macrophages to the M2 phenotype and accelerated the transition from the inflammatory to the proliferative phase (Fig. 7G and S13). On day 5, the GTMG hydrogel significantly increased the expression and dispersion of M2-type macrophages (CD206 and Arg1) and considerably decreased the expression of iNOS M1-type macrophages. On day 10, the Con group, which was still in the inflammatory phase, exhibited expression of M1-type macrophages (CD86and iNOS). In contrast, the wound in the GTMG hydrogel group progressed to the proliferative phase with a decrease in macrophage density. Macrophages play a significant role in the local immune response after tissue injury. The transition from pro-inflammatory (M1) to anti-inflammatory phenotype (M2) is improperly regulated in burn tissues, thereby slowing wound healing. The above results showed that GTMG hydrogel effectively stimulates the presence of a large number of M2 macrophages compared to the other groups, suggesting that GA should be the main component in inducing M2 macrophages. With the increase of M2 macrophages, anti-inflammatory cytokines or restorative growth factors are secreted, which changes the microenvironment of the wound tissue and facilitates the healing of burn wounds.

Compared with the Con and SSD groups, the GTMG hydrogel considerably accelerated wound healing, promoted the reconstruction of skin structure, aided blood-vessel regeneration, accelerated collagen deposition, and had a greater therapeutic effect on burn wounds. The excellent injectability, shape adaptability, and adhesion properties of the GTMG hydrogel enabled its application to burn sites with high-frequency movement, such as the groin and joints. These results indicated that the GTMG hydrogel has great potential for treating burn wounds.

4. Conclusions

In this study, we developed an injectable, strongly adhesive, shape-adaptable multifunctional hydrogel dressing, GTMG, to promote burn wound healing and tissue regeneration. The GTMG hydrogel can stimulate the transformation of macrophages from the M1 phenotype to the M2 phenotype, reduce the expression of pro-inflammatory cytokines, promote collagen deposition, regulate the inflammatory microenvironment, and significantly accelerate wound healing. The combination of GA and TA endows GTMG with excellent antioxidant activity, as well as antibacterial and hemostatic properties. Moreover, GTMG not only has good biocompatibility but also can degrade *in vivo*, thus preventing damage to the skin during dressing changes. The incorporation of Mg^{2+} imparts good angiogenic properties to the hydrogel. *In vitro* and *in vivo* studies have shown that, compared with SSD dressings, the GTMG hydrogel shortens the wound-healing time and promotes the complete restoration of skin structure. In summary, the GTMG hydrogel significantly promotes burn wound healing by regulating macrophage phenotypes and reducing the inflammatory response. It shows significant potential in immunomodulation-related wound treatments and provides a promising approach for treating burn wounds.

CRediT authorship contribution statement

Erman Zhao: Writing – review & editing, Writing – original draft. **Xiuling Tang:** Methodology, Investigation. **Xitong Li:** Resources, Methodology. **Jun Zhao:** Methodology. **Saiying Wang:** Methodology. **Gaofei Wei:** Writing – review & editing, Funding acquisition, Conceptualization. **Le Yang:** Writing – original draft, Supervision, Funding acquisition, Conceptualization. **Minggao Zhao:** Writing – review & editing, Supervision, Funding acquisition, Conceptualization.

Declaration of competing interest

The authors declare that they have no known competing financial interests or personal relationships that could have appeared to influence the work reported in this paper.

Acknowledgments

This study was supported by the National Natural Science Foundation of China (No. 82221001, No. 32241007 and No. 82173682), and partially supported by Shanxi Province Key Industry Innovation Chain Project (Grant number 2023-ZDLSF-59), Shaanxi Youth Rising Stars in Science and Technology (No. 2024 ZC-KJXX-119).

Appendix A. Supplementary data

Supplementary data to this article can be found online at https://doi.org/10.1016/j.mtbio.2025.101686.

Data availability

Data will be made available on request.

References

[1] M. Stanojcic, R. Vinaik, M.G. Jeschke, Status and challenges of predicting and diagnosing sepsis in burn patients, Surg. Infect. 19 (2018) 168–175, https://doi.org/10.1089/sur.2017.288.

[2] M.W. Pletz, M. Bauer, A.A. Brakhage, One step closer to precision medicine for infectious diseases, Lancet Infect. Dis. 19 (2019) 564–565, https://doi.org/10.1016/S1473-3099(19)30070-2.

[3] Y.W. Wang, J. Beekman, J. Hew, S. Jackson, A.C. Issler-Fisher, R. Parungao, S. S. Lajevardi, Z. Li, P.K.M. Maitz, Burn injury: challenges and advances in burn wound healing, infection, pain and scarring, Adv. Drug Deliv. Rev. 123 (2018) 3–17, https://doi.org/10.1016/j.addr.2017.09.018.

[4] M.G. Jeschke, M.E. van Baar, M.A. Choudhry, K.K. Chung, N.S. Gibran, S. Logsetty, Burn injury, Nat. Rev. Dis. Primers 6 (2020) 11, https://doi.org/10.1038/s41572-020-0145-5.

[5] C.C. Finnerty, M.G. Jeschke, L.K. Branski, J.P. Barret, P. Dziewulski, D.N. Herndon, Hypertrophic scarring: the greatest unmet challenge after burn injury, Lancet 388 (2016) 1427–1436, https://doi.org/10.1016/S0140-6736(16)31406-4.

[6] J. Maitz, J. Merlino, S. Rizzo, G. McKew, P. Maitz, Burn wound infections microbiome and novel approaches using therapeutic microorganisms in burn wound infection control, Adv. Drug Deliv. Rev. 196 (2023) 114769, https://doi.org/10.1016/j.addr.2023.114769.

[7] H. Zhao, J. Huang, Y. Li, X. Lv, H. Zhou, H. Wang, ROS-scavenging hydrogel to promote healing of bacteria infected diabetic wounds, Biomaterials 258 (2020) 120286, https://doi.org/10.1016/j.biomaterials.2020.120286.

[8] A.B. Aurora, E.N. Olson, Immune modulation of stem cells and regeneration, Cell Stem Cell 15 (2014) 14–25, https://doi.org/10.1016/j.stem.2014.06.009.

[9] P.J. Hines, Rapid response to tissue damage, Science 363 (2019) 1296–1298, https://doi.org/10.1126/science.363.6433.1296-m.

[10] Z. Tu, M. Chen, M. Wang, Z. Shao, X. Jiang, K. Wang, Z. Yao, S. Yang, X. Zhang, W. Gao, Engineering bioactive M2 macrophage-polarized anti-inflammatory, antioxidant, and antibacterial scaffolds for rapid angiogenesis and diabetic wound repair, Adv. Funct. Mater. 31 (2021) 2100924, https://doi.org/10.1002/adfm.202100924.

[11] Y. Yuan, S. Shen, D. Fan, A physicochemical double cross-linked multifunctional hydrogel for dynamic burn wound healing: shape adaptability, injectable self-healing property and enhanced adhesion, Biomater. 276 (2021) 120838, https://doi.org/10.1016/j.biomaterials.2021.120838.

[12] L. Yang, M. Wang, Y. Guo, T. Sun, Y. Li, Q. Yang, K. Zhang, S.B. Liu, M.G. Zhao, Y. M. Wu, Systemic inflammation induces anxiety disorder through CXCL12/CXCR4 pathway, Brain Behav. Immun. 56 (2016) 352–362, https://doi.org/10.1016/j.bbi.2016.03.001.

[13] Q. Li, H. Song, S. Li, P. Hu, C. Zhang, J. Zhang, Z. Feng, D. Kong, W. Wang, P. Huang, Macrophage metabolism reprogramming EGCG-Cu coordination capsules delivered in polyzwitterionic hydrogel for burn wound healing and regeneration, Bioact. Mater. 29 (2023) 251–264, https://doi.org/10.1016/j.bioactmat.2023.07.011.

[14] S. Amini-Nik, Y. Yousuf, M. Jeschke, Scar management in burn injuries using drug delivery and molecular signaling: current treatments and future directions, Adv. Drug Deliv. Rev. 123 (2018) 135–154, https://doi.org/10.1016/j.addr.2017.07.017.

[15] Y. Wang, J. Beekman, J. Hew, S. Jackson, A.C. Issler-Fisher, R. Parungao, S. S. Lajevardi, Z. Li, P.K.M. Maitz, Burn injury: challenges and advances in burn wound healing, infection, pain and scarring, Adv. Drug Deliv. Rev. 123 (2018) 3–17, https://doi.org/10.1016/j.addr.2017.09.018.

[16] X. Wang, P. Wu, X. Hu, C. You, R. Guo, H. Shi, S. Guo, H. Zhou, Y. Chao, Y. Zhang, C. Han, Polyurethane membrane/knitted mesh-reinforced collagen–chitosan bilayer dermal substitute for the repair of full-thickness skin defects via a two-step procedure, J. Mech. Behav. Biomed. 56 (2016) 120–133, https://doi.org/10.1016/j.jmbbm.2015.11.021.

[17] K. Zhang, C. Yang, C. Cheng, C. Shi, M. Sun, H. Hu, T. Shi, X. Chen, X. He, X. Zheng, M. Li, D. Shao, Bioactive injectable hydrogel dressings for bacteria-infected diabetic wound healing: a “pull−push” approach, ACS Appl. Mater. Interfaces 14 (2022) 26404–26417, https://doi.org/10.1021/acsami.2c04300.

[18] S. Chen, H. Wang, J. Du, Z. Ding, T. Wang, L. Zhang, J. Yang, Y. Guan, C. Chen, M. Li, Z. Hei, Y. Tao, W. Yao, Near-infrared light-activatable, analgesic nanocomposite delivery system for comprehensive therapy of diabetic wounds in rats, Biomaterials 305 (2024) 122467, https://doi.org/10.1016/j.biomaterials.2024.122467.

[19] Y. Li, L. Yang, Y. Hou, Z. Zhang, M. Chen, M. Wang, J. Liu, J. Wang, Z. Zhao, C. Xie, Polydopamine-mediated graphene oxide and nanohydroxyapatite-incorporated conductive scaffold with an immunomodulatory ability accelerates periodontal bone regeneration in diabetes, Bioact. Mater. 18 (2022) 213–227, https://doi.org/10.1016/j.bioactmat.2022.03.021.

[20] M.H. Norahan, S.C. Pedroza-González, M.G. Sánchez-Salazar, M.M. Álvarez, G. Trujillo de Santiago, Structural and biological engineering of 3D hydrogels for wound healing, Bioact. Mater. 24 (2023) 197–235, https://doi.org/10.1016/j.bioactmat.2022.11.019.

[21] C.Y. Zou, X.X. Lei, J.J. Hu, Y.L. Jiang, Q.J. Li, Y.T. Song, Q.Y. Zhang, L.J. Li, H. Q. Xie, Multi-crosslinking hydrogels with robust bio-adhesion and pro-coagulant activity for first-aid hemostasis and infected wound healing, Bioact. Mater. 16 (2022) 388–402, https://doi.org/10.1016/j.bioactmat.2022.02.034.

[22] C. Hoyle, J. Rivers-Auty, E. Lemarchand, S. Vranic, E. Wang, M. Buggio, N. J. Rothwell, S.M. Allan, K. Kostarelos, D. Brough, Small, thin graphene oxide is anti-inflammatory activating nuclear factor erythroid 2-related factor 2 via metabolic reprogramming, ACS Nano 12 (2018) 11949–11962, https://doi.org/10.1021/acsnano.8b03642.

[23] J. Park, J. Jeon, B. Kim, M.S. Lee, J.Y. Lee, Electrically conductive hydrogel nerve guidance conduits for peripheral nerve regeneration, Adv. Funct. Mater. 30 (2020) 2003759, https://doi.org/10.1002/adfm.202003759.

[24] A. Joorabloo, T. Liu, Recent advances in reactive oxygen species scavenging nanomaterials for wound healing, Exploration 4 (2024) 20230066, https://doi.org/10.1002/EXP.20230066.

[25] N. Kharouf, D. Mancino, J. Zghal, S. Helle, H. Jmal, M. Lenertz, N. Viart, N. Bahlouli, F. Meyer, Y. Haikel, V. Ball, Dual role of tannic acid and pyrogallol incorporated in plaster of Paris: morphology modification and release for antimicrobial properties, Mater. Sci. Eng. C 127 (2021) 112209, https://doi.org/10.1016/j.msec.2021.112209.

[26] T.S. Sileika, D.G. Barrett, R. Zhang, K.H.A. Lau, P.B. Messersmith, Colorless multifunctional coatings inspired by polyphenols found in tea, chocolate, and wine, Angew. Chem. Int. Ed. Engl. 52 (2013) 10766–10770, https://doi.org/10.1002/anie.201304922.

[27] Z. Ahmadian, A. Correia, M. Hasany, P. Figueiredo, F. Dobakhti, M.R. Eskandari, S. H. Hosseini, R. Abiri, S. Khorshid, J. Hirvonen, H.A. Santos, M. Shahbaz, A hydrogen-bonded extracellular matrix-mimicking bactericidal hydrogel with radical scavenging and hemostatic function for pH-responsive wound healing acceleration, Adv. Healthcare Mater. (2020) 2001122, https://doi.org/10.1002/adhm.202001122.

[28] A. Shariati, S.M. Hosseini, Z. Chegini, A. Seifalian, M.R. Arabestani, Graphene-based materials for inhibition of wound infection and accelerating wound healing, Biomed. Pharmacother. 158 (2023) 114184, https://doi.org/10.1016/j.biopha.2022.114184.

[29] B. Lu, T. Li, H. Zhao, X. Li, C. Gao, S. Zhang, E. Xie, Graphene-based composite materials beneficial to wound healing, Nanoscale 4 (2012) 2978, https://doi.org/10.1039/c2nr11958g.

[30] K. Zhang, Z. Jia, B. Yang, Q. Feng, X. Xu, W. Yuan, X. Li, X. Chen, L. Duan, D. Wang, L. Bian, Adaptable hydrogels mediate cofactor-assisted activation of biomarker-responsive drug delivery via positive feedback for enhanced tissue regeneration, Adv. Sci. 5 (2018) 1800875, https://doi.org/10.1002/advs.201800875.

[31] Z. Guo, Z. Zhang, N. Zhang, W. Gao, J. Li, Y. Pu, B. He, J. Xie, A Mg^{2+}/polydopamine composite hydrogel for the acceleration of infected wound healing, Bioact. Mater. 15 (2021) 203–213, https://doi.org/10.1016/j.bioactmat.2021.11.036.

[32] X. Wei, W. Zhou, Z. Tang, H. Wu, Y. Liu, H. Dong, N. Wang, H. Huang, S. Bao, L. Shi, X. Li, Y. Zheng, Z. Guo, Magnesium surface-activated 3D printed porous PEEK scaffolds for in vivo osseointegration by promoting angiogenesis and osteogenesis, Bioact. Mater. 20 (2022) 16–28, https://doi.org/10.1016/j.bioactmat.2022.05.011.

[33] E. Zhao, H. Liu, Y. Jia, T. Xiao, J. Li, G. Zhou, J. Wang, X. Zhou, X.J. Liang, J. Zhang, Z. Li, Engineering a photosynthetic bacteria-incorporated hydrogel for infected wound healing, Acta Biomater. 140 (2022) 302–313, https://doi.org/10.1016/j.actbio.2021.12.017.

[34] E. Zhao, T. Xiao, Y. Tan, X. Zhou, Y. Li, X. Wang, K. Zhang, C. Ou, J. Zhang, Z. Li, H. Liu, Separable microneedles with photosynthesis-driven oxygen manufactory for diabetic wound healing, ACS Appl. Mater. Interfaces 15 (2023) 7725–7734, https://doi.org/10.1021/acsami.2c18809.

[35] X. Zhao, S. Li, X. Du, W. Li, Q. Wang, D. He, J. Yuan, Natural polymer-derived photocurable bioadhesive hydrogels for sutureless keratoplasty, Bioact. Mater. 8 (2022) 196209, https://doi.org/10.1016/j.bioactmat.2021.07.001.

[36] W. Zhao, Y. Li, X. Zhang, R. Zhang, Y. Hu, C. Boyer, F.J. Xu, Photo-responsive supramolecular hyaluronic acid hydrogels for accelerated wound healing, J. Control Release 323 (2020) 24–35, https://doi.org/10.1016/j.jconrel.2020.04.014.

[37] C. Li, C. Guo, V. Fitzpatrick, A. Ibrahim, D.L. Kaplan, Design of biodegradable, implantable devices towards clinical translation, Nat. Rev. Mater. 5 (2020) 61–81, https://doi.org/10.1038/s41578-019-0150-z.

[38] Z. Qiao, X. Lv, S. He, S. Bai, X. Liu, L. Hou, J. He, D. Tong, R. Ruan, J. Zhang, J. Ding, H. Yang, A mussel-inspired supramolecular hydrogel with robust tissue anchor for rapid hemostasis of arterial and visceral bleedings, Bioact. Mater. 6 (2021) 2829–2840, https://doi.org/10.1016/j.bioactmat.2021.01.039.

[39] M. Dong, Y. Mao, Z. Zhao, J. Zhang, L. Zhu, L. Chen, L. Cao, A novel double-crosslinking-double-network design for injectable hydrogels with enhanced tissue adhesion and antibacterial capability for wound treatment, Adv. Funct. Mater. 30 (2020) 1904156, https://doi.org/10.1002/adfm.201904156.

[40] H. Ren, Z. Zhang, X. Cheng, Z. Zou, X. Chen, C. He, Injectable, self-healing hydrogel adhesives with firm tissue adhesion and on-demand biodegradation for sutureless wound closure, Sci. Adv. 9 (2023) eadh4327, https://doi.org/10.1126/sciadv.adh4327.

[41] G. Huang, F. Li, X. Zhao, Y. Ma, Y. Li, M. Lin, G. Jin, T. Lu, G.M. Genin, F. Xu, Functional and biomimetic materials for engineering of the three-dimensional cell microenvironment, Chem. Rev. 117 (2017) 12764–12850, https://doi.org/10.1021/acs.chemrev.7b00094.

[42] N. Ninan, A. Forget, V.P. Shastri, N.H. Voelcker, A. Blencowe, Antibacterial and anti-inflammatory pH-responsive tannic acid-carboxylated agarose composite

hydrogels for wound healing, ACS Appl. Mater. Interfaces 8 (2016) 28511–28521, https://doi.org/10.1021/acsami.6b10491.
[43] D.J. Munoz-Pinto, V.R. Guiza-Arguello, S.M. Becerra-Bayona, E.M. Josh, S. Satyavrata, M. Sarah, R. Brooke, H. Magnus, S.H. Mariah, Collagen-mimetic hydrogels promote human endothelial cell adhesion, migration and phenotypic maturation, J. Mater. Chem. B 3 (2015) 7912–7919, https://doi.org/10.1039/C5TB00990A.
[44] D. Missirlis, J.P. Spatz, Combined effects of PEG hydrogel elasticity and celladhesive coating on fibroblast adhesion and persistent migration, Biomacromolecules 15 (2014) 195–205, https://doi.org/10.1021/bm4014827.
[45] R.J. Waddington, R. Moseley, G. Embery, Reactive oxygen species: a potential role in the pathogenesis of periodontal diseases, Oral Dis. 6 (2000) 138–151, https://doi.org/10.1111/j.1601-0825.2000.tb00325.x.
[46] N. Sahiner, Self-crosslinked ellipsoidal poly(tannic acid) particles for bio-medical applications, Molecules 26 (2021) 2429, https://doi.org/10.3390/molecules26092429.
[47] N. Sahiner, S. Sagbas, N. Aktas, C. Silan, Inherently antioxidant and antimicrobial tannic acid release from poly(tannic acid) nanoparticles with controllable degradability, Colloid Surface. B. 142 (2016) 334–343, https://doi.org/10.1016/j.colsurfb.2016.03.006.
[48] Y. Huang, X. Zhao, Z. Zhang, Y. Liang, Z. Yin, B. Chen, L. Bai, Y. Han, B. Guo, Degradable gelatin-based IPN cryogel hemostat for rapidly stopping deep noncompressible hemorrhage and simultaneously improving wound healing, Chem. Mater. 32 (15) (2020) 6595–6610, https://doi.org/10.1021/acs.chemmater.0c02030.
[49] L. Deng, Y. Qi, Z. Liu, Y. Xi, W. Xue, Effect of tannic acid on blood components and functions, Colloids Surface. B. 184 (1) (2019) 110505, https://doi.org/10.1016/j.colsurfb.2019.110505.
[50] V. Falanga, Wound healing and its impairment in the diabetic foot, Lancet 366 (2005) 1736–1743, https://doi.org/10.1016/S0140-6736(05)67700-8.
[51] B. Zhang, J. He, M. Shi, Y. Liang, B. Guo, Injectable self-healing supramolecular hydrogels with conductivity and photo-thermal antibacterial activity to enhance complete skin regeneration, Chem. Eng. J. 400 (2020) 125994, https://doi.org/10.1016/j.cej.2020.125994.
[52] C. Wang, Q. Wang, W. Gao, Z. Zhang, Y. Lou, H. Jin, X. Chen, B. Lei, H. Xu, C. Mao, Highly efficient local delivery of endothelial progenitor cells significantly potentiates angiogenesis and full-thickness wound healing, Acta, Biomater 69 (2018) 156–169, https://doi.org/10.1016/j.actbio.2018.01.019.